Publications of the Astronomical Society of the Pacific
95:451-456, July 1983

ANALYSIS OF MOUNT ST. HELENS ASH FROM OPTICAL PHOTOELECTRIC PHOTOMETRY

J. A. CARDELLI

Department of Astronomy, FM-20, University of Washington, Seattle, Washington 98195

AND

T. P. ACKERMAN

NASA-Ames Research Center, Mail Stop 245-3, Moffet Field, California 94035

Received 1983 March 7

The properties of Mount St. Helens ash have been discussed in many previous papers. However, these analyses involved measurements of samples obtained on the ground or in the air. This paper involves using data from optical photoelectric observations of standard stars taken 48 hours after the UT 1980 July 23 eruption of Mount St. Helens which yielded optical properties of the suspended dust particles. The analysis of the data centers on the use of Mie theory for determining the mean particle size and the column density of the particles in the extincting layer. Although this method relies on choosing a particle-size distribution, the wavelength dependance of the optical extinction seems most sensitive to the mean particle size and not the type of distribution. However, the computed column density varies by as much as a factor of ten depending on the type of distribution used. The extinction probably arose from suspended ash at low altitudes which slowly migrated over the site during the 48-hour period following the eruption. Since our determined mean particle size (0.18 micron) is similar to what is found for urban pollutant aerosols, the extincting material may in part be the result of gas-to-particle conversion within the volcanic plume.

Key words: photometry—atmospheric extinction—volcanic ash—Mie scattering

I. Introduction

Manastash Ridge Observatory run by the University of Washington, Department of Astronomy, is located 16 km southwest of Ellensburg, Washington, and is on a trajectory of about 160 km east-northeast of Mount St. Helens. The eruption of UT 1980 July 23 resulted in ash fallout at the site. However, an inspection of conditions prior to observing on UT 1980 July 25 did not indicate anything that would have lead us to expect anomalous extinction and so a program of photoelectric photometry was carried out. Included in this program, for the purpose of determining atmospheric extinction, was a set of standard stars of known intrinsic (above the atmosphere) colors and magnitudes. It was through the reduction of these standard stars that the anomalous extinction was determined. As will be seen, this anomalous extinction appeared as an additional extinction component above what is normally considered to be the standard (or normal) site extinction. In addition, we were able to determine the amount of this additional extinction because the extinction that is normal for our observing site was well determined during the 1980 observing season.

II. Observations and Reductions

The photoelectric observations were obtained with the University of Washington 0.76-meter telescope. The photoelectric system (the Washington system) consists of five broad-band filters typically several hundred angstroms wide coupled with a dry-ice-cooled Ga-As phototube. The effective wavelengths of the filters, λ_{eff}, appear in Table I. Details concerning the system can be found in Canterna (1976), Canterna and Harris (1979), and Harris and Canterna (1979).

The reduction of the observed data consists of two phases. The first involves reducing the observed intensities, I_λ, into colors and magnitudes via equations (1) and (2), respectively

$$M_{\lambda_j} - M_{\lambda_k} = 2.5 \log(I_{\lambda_k}/I_{\lambda_j}) \quad (1)$$

$$M_{\lambda_j} = -2.5 \log I_{\lambda_j} \quad . \quad (2)$$

To determine the atmospheric extinction, several observations of standard stars covering a wide range in color are obtained over a large range in air mass. Air mass, X, is defined as the absorbing thickness of the atmosphere

Table I

Extinction Data From UT 7/25/80

Filter	λ_{eff} (Å) ($\times 10^{-8}$ cm)	λ_{eff}^{-1} (μ^{-1}) ($\times 10^4$ cm^{-1})	A_λ (Mag/Airmass)							
			Observed			Normal$_d$		Anomalous Extinction (Observed-Normal)		
			1_a	2_b	σ_c		σ	1_a	2_b	σ
C	3910	2.56	.720	1.017	.009	.484	.009	.236	.533	.013
M	5085	1.97	.410	.655	.008	.215	.008	.195	.440	.011
V	5480	1.83	.360	.580	.005	.189	.006	.171	.391	.008
T1	6330	1.58	.273	.448	.007	.137	.007	.136	.311	.010
T2	8050	1.24	.144	.260	.009	.076	.009	.080	.184	.013

a—Data before 7:00 UT.
b—Data after 8:30 UT.
c—From mean errors for colors.
d—From 11 nights: 4/80-9/80.

where X is a function of the angle from the zenith normalized so that $X = 1$ at the zenith. Once the color and magnitude (in this case the V filter) extinction is determined, assumed by definition to be linear with air mass (the details of the reduction procedure can be found in Hardie (1962)), the observed data are corrected for the effects of atmospheric extinction. Since the filters are fairly broad, primary as well as color-dependent second-order extinction corrections must be applied since different stellar flux distributions will shift λ_{eff}. The extinction data used in this analysis are the primary extinction which corresponds to the filter's effective wavelength independent of the flux distribution (see Hardie 1962).

The second phase of the reduction consists of computing a linear transformation between the extinction-corrected data and the known intrinsic colors and magnitudes by which the photometric system is defined. In this way subtle differences between the system being used and the standard system can be accounted for. Typically, these coefficients are relatively constant for any one particular system. For our system, the dispersion of the transformation coefficients for eleven observing nights spanning several months before and after the UT 1980 July 25 observations reflect a variation from the mean of a few percent or less. Since our system seems stable and the transformation is independent of the extinction, any variations from the established system coefficients will be due to improper extinction corrections. Our reductions showed no such variations. Also, in principle it is possible to assume the mean coefficients discussed above and work backwards to find the extinction for each observation. The extinction determined in this way agrees with the values determined by the standard reduction method previously discussed.

The final data reduction not only indicated extinction that was significantly larger than the standard values for the site but also showed an abrupt systematic change over the course of the night. Standard stars observed before 7:00 UT yielded a set of extinction coefficients significantly smaller than for those stars observed after 8:30 UT. This change in the extinction layer must have occurred quite rapidly since extinction variations as a function of air mass for each time regime showed no deviations from the standard linear air mass dependence assumed in the reductions. To avoid systematic errors, data from each half of the night were corrected with their respective extinction values but both halves were transformed together. Since the transformation not only showed no systematic effects in the data as a function of air mass for either half but also yielded transformation coefficients consistent with the mean system values discussed above, the determined values should accurately represent the atmospheric extinction/air mass. The extinction data for each of the five wavelengths for each half of the night (labeled 1 and 2, respectively) appear in Table I along with the "normal" atmospheric extinction established during the months before and after our observations. The monocromatic values were determined from the differential (color) extinction via the V filter ($\lambda_{eff} = 5480$ Å) extinction.

III. Analysis

Atmospheric extinction in magnitudes is related to the change in intensity of the observed source as the light is transmitted through the extinction layer by the relation

$$A_\lambda = 2.5 \log(I_\lambda{}^0/I_\lambda) \quad , \tag{3}$$

which in turn is related to the wavelength-dependent particle cross-section and column density (single particle size) via

$$I_\lambda/I_\lambda{}^0 = \exp(-\tau) = \exp(-S_\lambda N) \quad , \tag{4}$$

where

$I_\lambda{}^0$ is the monocromatic intensity above the atmosphere,
I_λ is the observed intensity
S_λ is the wavelength dependent particle cross-section (cm^2)
N is the particle column density (cm^{-2}), and
τ is the optical depth of the extincting layer.

For a distribution of particle sizes, $S_\lambda N$ in equation (4) is replaced with the integral of $S_{\lambda,a}N_a$ (both dependent on size) over the particle radius, a.

Because the extinction is measured in magnitudes, the anomalous extinction due solely to the volcanic ash can be found by subtracting the "normal" site extinction from the observed values. The resulting anomalous extinction along with the observed and normal site data can be found in Table I. The general Rayleigh nature of the normal site extinction is clearly indicated by the fit of these data with an arbitrary linear λ^{-4} relation (see left side of Fig. 1). Also, it is immediately evident from the middle plot in Figure 1 that the ash particles are of the order of a few tenths of a micron in size since in general the wavelength of the turnover of the extinction is related to the mean particle size (Greenberg 1968). From equations (3) and (4), the relationship of the particle extinction, A_λ, to the size-dependent parameters is given by

$$A_\lambda = 1.086\, S_\lambda N \quad . \tag{5a}$$

For a distribution of particle sizes, the relation is given by

$$A_\lambda = 1.086 \int_0^\infty S_{\lambda,a} N_a da \tag{5b}$$

where

$$N = \text{total column density} = \int_0^\infty N_a da \quad .$$

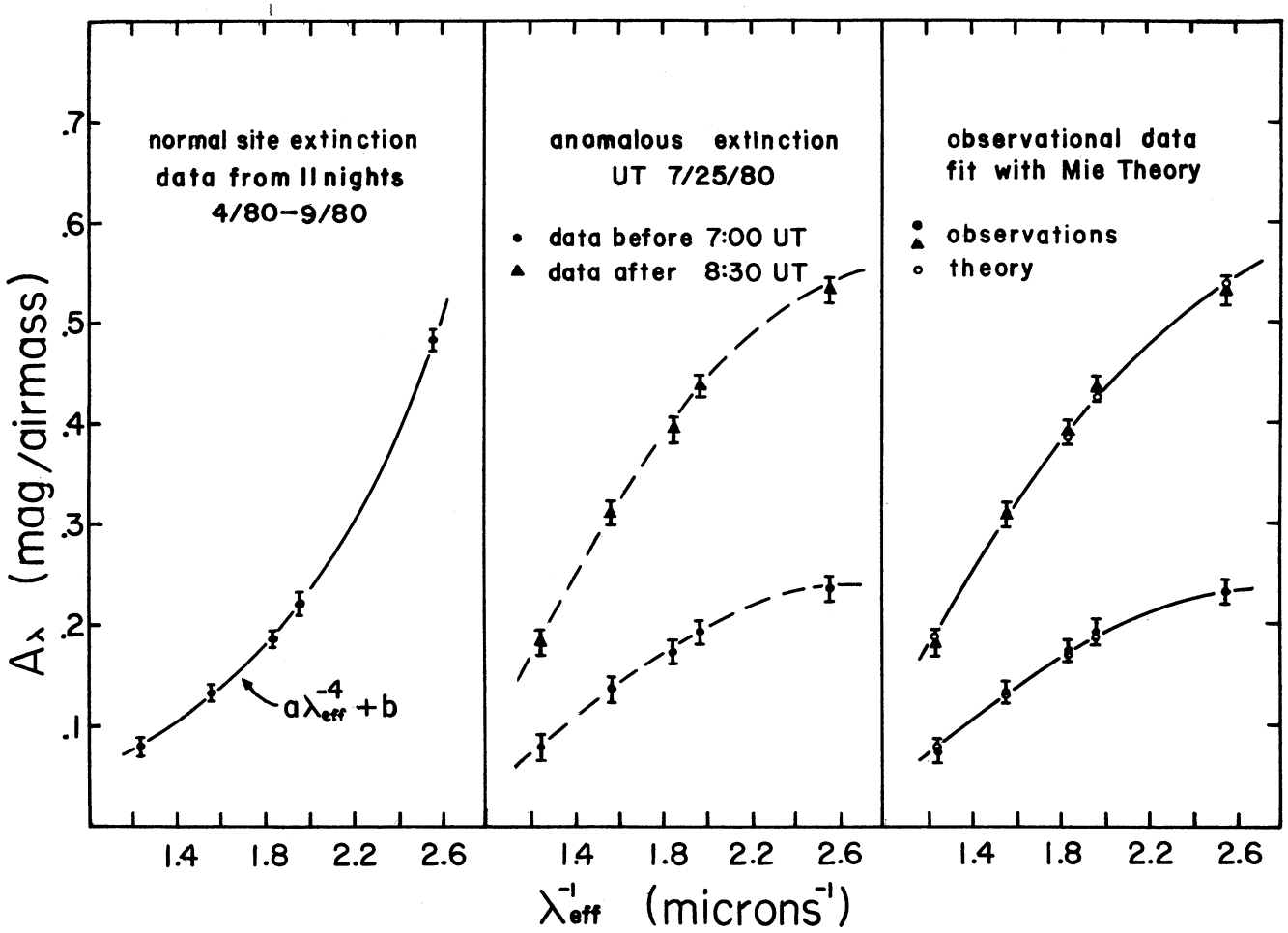

FIG. 1—Extinction data. Normal site extinction (left panel); Anomalous extinction due to volcanic ash on UT 1980 July 25 (middle panel); Fit of the anomalous extinction with the data from Tables II and III using equation (7) (left panel).

The standard notation for Mie theory (see Wickramasinghe 1967, 1973) involves the use of the normalized extinction efficiency factor, Q_λ^{ext}, where $Q_\lambda^{ext} = S_\lambda/\pi a^2$. Thus alternate forms of equations (5a) and (5b) are found by replacing S_λ with $Q_\lambda^{ext}\,\pi a^2$.

Since S_λ (or Q_λ^{ext}) depends upon the particle radius, a, and the complex refractive index, $m = n - ki$, any resulting fit of the observed data with Mie theory will not necessarily be unique. An equally satisfactory fit can be found for either silicates (Wickramasinghe 1973; $m \sim 1.6 - 0.01\,i$) or graphite (Wickramasinghe and Guillaume 1965; $m \sim 2.5 - 1.5\,i$) but the resulting mean particle sizes differ by a factor of 2 to 3. We must note that graphite was chosen as an example only because the data are readily available. However, the problem of fixing the index of refraction is actually not as difficult as it might seem since measured values for Mount St. Helens ash from previous eruptions prior to UT 1980 July 23 are available in the literature. As might be expected, the values reflect that of silicate particles and are in the range $m \sim (1.5 - 1.6) - (0.002 - 0.004)i$ (Patterson 1981) for the wavelength range we studied. Although no values were specifically measured for the UT 23 July ash, the ash is overall quite similar in appearance to previous eruptions (UT 18 May for example). In addition, the X-ray spectrum taken on an energy-dispersive spectrometer indicates the strong presence of silicon as well as aluminum, calcium, and potassium for a sample of the UT 23 July and UT 18 May eruptions. Finally, as will be seen, slight variations in n and k (few percent) result in no apparent change in the extinction fit for a given mean particle size. We therefore feel safe in assuming the above range in m as being representative of our sample.

Equation (5b) is handled easily by normalizing the right-hand side by

$$\langle S_\lambda \rangle = \int_0^\infty S_{\lambda,a} N_a da \Big/ \int_0^\infty N_a da \quad . \tag{6}$$

Thus equation (5b) reduces to

$$\log A_\lambda = \log\langle S_\lambda \rangle + \log[1.086 \int_0^\infty N_a da] \quad . \tag{7}$$

Using Mie theory (see Wickramasinghe 1973) and a chosen particle-size distribution, values of $\langle S_\lambda \rangle$ can be computed. The distribution used in this analysis was log-normal of the form

$$N_a \propto \exp[-(\ln a - \ln \langle a \rangle_n)^2 / 2 \ln^2 \sigma] \quad , \qquad (8)$$

where $\langle a \rangle_n$ is the number geometric mean particle radius and σ is the geometric standard deviation of the distribution. This distribution, along with $\sigma = 2$, was used because it is often observed in nature (Butcher and Charlson 1972). In fact, physical measurements of ash sizes from preceeding eruptions strongly indicate log-normal particle-size distributions (Chuan, Woods, and McCormick 1981; Farlow et al. 1981).

We must note that the mean radius used in this analysis is actually $\langle a \rangle_v$, the volume geometric mean radius which is related to $\langle a \rangle_n$ by $\langle a \rangle_v = \langle a \rangle_n \exp(3 \ln^2 \sigma)$. This is because the volume weighted mean is closer to what the photon actually "sees" than simply the particle cross-section. Thus the mean size actually responsible for determining the shape of the observed extinction is shifted slightly away from the peak of number distribution ($\langle a \rangle_n$). Consequently, any further reference to the mean radius will correspond to $\langle a \rangle_v$ which we simply denote by $\langle a \rangle$.

Table II contains the final best-fit values of $\langle S_\lambda \rangle$ found from adjusting $\langle a \rangle$ (see eq. (6)) till good agreement was found with the observed data as seen in equation (7). The estimated uncertainty in $\langle a \rangle$ is of the order of 10%. Once the shape of the observed extinction has been fit in this way, the constant on the right-hand side of equation (7) can be determined, and the column density calculated for each point. The mean column density determined from the data along with the determined mean particle size for the log-normal distribution appears in Table III. The dispersion in the fifth column is based on the scatter about the fit only and assumes no uncertainty in the data. The dispersion in the sixth column includes the uncertainty in the data and although more realistic, it is not much different. The final fit of the observed anomalous extinction from Table I with the best-fit values of $\langle S_\lambda \rangle$ (Table II) and the column density (Table III) as determined from equation (7) appears in the right half of Figure 1.

Table II

Model Extinction Cross-Sections[a]

Filter	$Q_\lambda^{ext} \pi a^2$ Single Size $a_0 = .18\mu$	$\langle S_\lambda \rangle$ Log-Normal Distribution $\bar{a} = .18$
C	3.69×10^{-1} μ^2	2.13×10^{-2} μ^2
M	2.80×10^{-1} "	1.68×10^{-2} "
V	2.58×10^{-1} "	1.52×10^{-2} "
T1	2.01×10^{-1} "	1.23×10^{-2} "
T2	1.11×10^{-1} "	7.41×10^{-3} "

[a] See text

The sensitivity of the type of size distribution was tested by using the data of Wickramasinghe (1973) and computing a best fit for a single particle size ($a = \langle a \rangle = a_0$) and for an arbitrary Gaussian distribution. The best fit values of a_0 and N (column density) for the single size also appear in Table III. In both cases, $\langle a \rangle$ remains the same within the data uncertainty although the column densities are understandably different. It therefore appears that the shape of the extinction is most sensitive to the mean size and only slightly dependent on the number distribution of sizes different from the mean. However, the fact that these other particles contribute slightly to the overall extinction (but not the shape) explains the variations in the column densities. Also, as stated earlier, the fit seems reasonably insensitive to small variations in m. The imaginary part of the refractive index for the single size fit was about a factor ten larger than for the log-normal distribution but resulted in no apparent change in $\langle a \rangle$. A fit using $m = 1.5 - 0.05i$ also yielded the same $\langle a \rangle$ although the column density was about 25% different. Thus, slight variations of m and the size distribution seem to put a range on the column density of the order of a factor of 2–20 while there seems to be an effect on $\langle a \rangle$ of only a few percent (the uncertainty in the fit itself).

IV. Discussion

One obvious conclusion from this analysis is that the ash layer underwent a fairly rapid change during the course of the observations on UT 25 July, apparently increasing in number density by a factor of about two. Extinction data for individual stars for both halves of the night showed no noticable spatial variation. Thus, the increase in ash must have occurred fairly rapidly between 7:00 and 8:30 UT since the extinction layer appeared

Table III

Column Density (N) Through the Extinction Layer for UT 7/25/80

	Distribution	Mean Size	$N(cm^{-2})$	$\sigma_a(cm^{-2})$	$\sigma_b(cm^{-2})$
Data Before	Single Size	$a_0 = .18\mu$	6.25×10^7	0.29×10^7	0.50×10^7
7:00 UT	Log-Normal	$\bar{a} = .18\mu$	1.02×10^9	0.03×10^9	0.08×10^9
Data After	Single Size	$a_0 = .18\mu$	1.43×10^8	0.07×10^8	0.05×10^8
8:30 UT	Log-Normal	$\bar{a} = .18\mu$	2.33×10^9	0.07×10^9	0.08×10^9

[a] Scatter about the fit - assumes no scatter in data.
[b] Including scatter in the data - see Table 1.

uniform for each time regime. The wind velocity measured at the site (1200-m elevation) increased from around 5 km hr^{-1} to about 15 km hr^{-1} during this transition period. If the wind velocity in the layer containing the ash also underwent such a change, it seems reasonable that additional ash or simply a larger portion of the "cloud" could have been introduced in a relatively short time. To understand this change, however, we must first try to understand the circumstances surrounding the initial migration of the ash.

Initially, it is not clear how the ash from the UT 23 July eruption could have remained so long in the region. Although it seems likely that particles of tenths of a micron or less in size could remain suspended for days, the eastward air flow should have carried most of the debris past the site by the time of the observations. For the period of UT 23 July to UT 25 July, the air flow between 3000 m and 12,000 m was west to east with a minimum velocity of about 15 km hr^{-1}. With the bulk of the plume being below 18,000 m, it seems likely that all of the material in this layer would have been swept past the site long before the time of the observations. Turbulence in this layer could have slowed the eastward migration of a small amount of the original plume but this cannot be confirmed.

A second, and more likely, possibility exists for the migration of ash in the layer 1500 m–3000 m. The air flow in this layer for the period UT 23 July to UT 25 July was in somewhat of a north-south loop between St. Helens and the Cascade Mountains to the east. Turbulence at these low altitudes especially over rough terrain, which is quite common, could easily have kept the ash suspended while the 2000-m mountains to the east acted as a barrier to slow the eastward migration. A subsequent increase in wind velocity late on UT 25 July could have increased the migration rate of a larger portion of the material creating the observed increase in the extinction after 8:30 UT.

A third, although unlikely, possibility exists for the reintroduction of ash into the airflow. Strong thermal updrafts to the west of the observatory could have resulted in particles being re-injected into the atmosphere at low altitudes. Such behavior frequently occurs during the summer months in the dry desert-like areas to the east of the observing site although quantitative measurements have never been made. However, sub-micron size particles of Mount St. Helens ash probably have a large sticking coefficient (especially if they have undergone gas-to-particle conversion). It therefore seems unlikely that a large enough quantity could be re-introduced in this way, although some contribution cannot be totally discounted.

The volume mean particle radius determined from our extinction measurements (0.18 micron) is somewhat smaller than that usually associated with volcanic-ash distributions. Instead, a volume mean radius of about this order is more typical of the size associated with urban pollutant aerosols (about 0.12 micron). Since these aerosols are usually associated with gas-to-particle conversion and subsequent coagulation (Butcher and Charlson 1972), the small size of the particles in our cloud suggests that, in this case, the volcanic aerosols may actually be composed of particles formed by conversion of sulfur gases in the plume. This would be consistent with the UT 23 July eruption which was fairly small and relatively lower in ash content than previous eruptions. The ash cloud measured at the observatory may also have included larger particles, but extinction at visible wavelengths would be dominated by the more abundant smaller particles. Also, if migration during the 48 hours after the eruption did occur in the layer below 3000 m (which seems most likely), many of the larger particles may have settled out.

If the particles producing the extinction were produced from gaseous precursers, their most likely composition would be sulfuric acid or ammonium sulfate. These substances have a real index of refraction, n, between 1.33 and 1.55, depending on the chemical form and the amount of water present, and an imaginary index of refration, k, of approximately zero. The use of these values would not affect our determination of the mean size to any great degree since it is dominated by n rather than k and as we have shown, slight variations in these values do indeed have little effect.

V. Summary

Measurements of the extinction properties of volcanic ash from the UT 23 July eruption of Mount St. Helens have allowed us to determine the optical properties of the suspended material. This was accomplished by using standard astronomical techniques associated with the reduction of broad-band photoelectric photometry of standard stars of known intensities. By assuming a refractive index, which has been previously determined for Mount St. Helens ash, we were able to determine the mean particle radius for a log-normal distribution of particles. This result is of interest because it appears that the particles of mean size ($\langle a \rangle$) are responsible for determining the shape of the observed wavelength-dependent extinction. In fact, the determination of the mean radius seems quite insensitive to the choice of the size distribution. While the column density is strongly dependent on the type of distribution used, the choice of the log-normal distribution, which naturally occurs quite often, allows a realistic determination of the density through the extinction layer. Although the exact nature of the presence of this material 48 hours after the eruption is uncertain, it most likely is related to the migration of particles below

3000 m. This may make it possible to put limits on the settling rate of the ash when compared to the initial populations at the time of the eruption. Although this information is not known for the UT 23 July eruption, comparisons with measurements from previous eruptions may provide a starting point.

The possibility also exists that the observed extinction resulted from gas-to-particle conversions in the material in the layer below 3000 m. Although this probably would have little effect on our determination of the mean size and the column density of the material, its presence 48 hours after the eruption may be more easily understood. It is possible that post-eruption outgassing could have helped supply the material necessary for this gas-to-particle conversion.

We would like to thank V. V. Smith for his help with the observations, H. Harris for his help with the data reduction, R. Canterna and N. Suntzeff for their helpful discussions and critical comments, and W. Spiesman for his finesse with computers and other electronic gadgets.

REFERENCES

Butcher, S. S., and Charlson, R. J. 1972, *An Introduction to Air Chemistry* (New York: Academic Press), pp. 165–79.

Canterna, R. 1976, *A.J.* 81, 228.

Canterna, R., and Harris, H. 1979, in *Problems of Calibration of Multicolor Photometric Systems, Dudley Obs. Reports* No. 14, A. G. H. Phillips, ed. (Schnectady, NY: Dudley Observatory), p. 199.

Chuan, R. L., Woods, D. C., and McCormick, M. P. 1981, *Science* 211, 830.

Farlow, N. H., Oberbeck, V. R., Snetsinger, K. G., Ferry, G. V., Polkowski, G., and Hayes, D. M. 1981, *Science* 211, 832.

Greenberg, J. M. 1968, in *Nebulae and Interstellar Matter*, B. A. Middlehurst and L. H. Aller, eds. (Chicago: University of Chicago Press), chap. 6.

Hardie, R. 1962, in *Astronomical Techniques*, W. A. Hiltner ed. (Chicago: University of Chicago Press), chap. 8.

Harris, H., and Canterna, R. 1979, *A.J.* 84, 1750.

Patterson, E. M. 1981, *Science* 211, 836.

Wickramasinghe, N. C. 1967, in *Interstellar Grains*, B. Lovell and Z. Kopal, eds. (London: Chapman and Hall Ltd.), chap. 2.

Wickramasinghe, N. C. 1973, *Light Scattering Functions for Small Particles* (London: Adam Hilger Ltd.).

Wickramasinghe, N. C., and Guillaume, C. 1965, *Nature* 207, 366.